Lasers in Manufacturing Conference 2017

Manufacturing, microstructure and mechanical properties of selective laser melted Ti6Al4V-Cu

A. Kinnear [a], T. C. Dzogbewu [a], P. Krakhmalev [b,*], I. Yadroitsava [a], I. Yadroitsev [a]

[a] Central University of Technology, Free State, Department of Mechanical and Mechatronic Engineering, Private Bag X20539, Bloemfontein 9300, South Africa
[b] -Karlstad University, Department of Mechanical and Materials Engineering, SE-651 88 Karlstad, Sweden

Abstract

Ti6Al4V is a commonly used biomedical alloy because of its suitable mechanical and biocompatible properties. Infection at the bone–implant interface is the most probable reason for implant failure directly after implantation. Copper is a proven anti-bacterial agent and in small amounts is not toxic to the human body. Copper additions reduce the risk of bacterial infection and implant failure. Thus advanced implants can be constructed to have a biocompatibility and antibacterial properties. Optimal process parameters are needed to be established for in-situ alloying of Ti6Al4V-Cu to form dense parts with suitable mechanical properties. The effect of laser scanning speeds and hatch distance on morphology of single layers was investigated. The surface roughness, chemical composition and distribution of Cu near the surface and within the synthesized layer, as well as micro hardness were considered. An employed rescanning strategy showed improved alloy homogeneity and surface quality. On the base of these data 3D samples were produced. Microstructure and mechanical properties of as-built parts were analysed.

Keywords: Ti alloys; implants; antibacterial properties; microstructure

1. Introduction

Ti6Al4V Extra Low Interstitials (ELI) is a commonly used biomaterial because of it suitable mechanical and biocompatible properties (Niiomi, 2008). Nevertheless, there is still a risk of failure of the titanium implants due to infection. Infection at the bone–implant interface is the most probable reason for implant failure

* Corresponding author. Tel.: +46(0)547002036;
E-mail address: pavel.krakhmalev@kau.se

directly after implantation (Geetha *et al.,* 2009). Medication can help to cure infection. Nevertheless, utilization of materials with embedded antibacterial properties is more efficient as they act locally and permanently at the site of infection. For example, coating of the implant interface with materials that have antibacterial properties is a promising approach to prevent occurrence of the infection and the bone-implant interface. Several metals like silver, zinc and copper have shown such antibacterial properties.

Copper is a proven antibacterial agent and in small amounts is not toxic to the human body (Nan *et al.*, 2008). To show the effect of Cu as an antibacterial agent, Jung *et al.* (2014) have electrochemically deposited small amounts of Cu onto Ti discs. After 10 days of exposure to the Cu, *Escherichia coli (E. coli)* and *Staphylococcus aureus (S. aureus)* bacteria have experienced a dramatic decrease in growth. Antibacterial functionalization of Ti implants by Cu also has been suggested by Shirai *et al.* (2009), who has used a Ti-Cu alloy as an implant with antibacterial properties. It has been indicated that 1% Cu addition retained the samples biocompatibility and inhibited the growth of bacterial microbes.

The medical industry has successfully utilized the layer-by-layer nature of Direct Metal Laser Sintering (DMLS) to manufacture complex shapes from biocompatible materials to produce implants using CAD geometry based on computer tomography scan data. Additionally, this technology combines advantages of powder metallurgy with complete melting of powder mixtures. It provides a unique opportunity to manufacture custom shapes and design new alloys with compositions impossible for conventional methods.

DLMS in-situ alloying from elemental powders is an attractive and economical means of manufacturing complex novel alloys. Vrancken *et al.* (2014) highlighted the capabilities of DMLS to in-situ processing of powder mixtures Ti6Al4V (ELI) and 10 wt.% Mo powders. Krakhmalev & Yadroitsev (2014) showed that an increase in laser power or a re-melting strategy are effective methods of improving homogeneity of in-situ DMLS Ti/SiC intermetallic materials. Fischer *et al.* (2016) produced Ti–26Nb alloy by DMLS of elemental titanium and niobium mixed powders, noting that energy input has a significant effect on porosity and homogeneity of the produced part. Dadbakhsh & Hao (2014) formed an in-situ DMLS Al-5 wt.%Fe_2O_3 alloy and showed that the layer thickness had a strong influence on the microstructural outcome.

This, in-situ alloying during DMLS approach could be efficiently applied to manufacturing of custom implants. A custom implant can be constructed to have a biocompatible Ti6Al4V structure with Cu additions at the bone–implant interface aimed to reduce the risk of bacterial infection and implant failure. In a pilot study by Kinnear *et al.* (2015) compared in-situ alloyed DMLS Ti6Al4V-1at.%Cu and a surface that had pure Cu areas on a Ti6Al4V substrate so that the surface contains 1% Cu by means of surface area. Results showed that the in-situ alloyed DMLS Ti6Al4V-1at.%Cu was efficient in inhibiting the growth of *E. coli* and *S. aureus*.

In-situ alloying during DMLS is challenging since a combination of good chemical homogeneity and high quality of the final 3D object is required. Fundamentally, the DMLS process is a laser beam scanning over the surface of a thin powder layer and melts it. Optimization of formation of the molten pool and single track plays a major role in the quality and mechanical properties of the manufactured 3D object. Process of a single track formation is directly influenced by the process parameters. At optimal process-parameters, DMLS single tracks are continuous and have stable geometrical characteristics. High energy input can lead to keyhole mode resulting in deep re-melting of the substrate and pores inside the molten pool (Yadroitsev *et al.*, 2012; Yadroitsava *et al.*, 2015). At low laser power density and high scanning speed, the molten pool has lower temperature, so the surface tension coefficient, as well as melt viscosity, increases and can lead to drop formation (Yadroitsev, 2009). For the in-situ alloying approach, the molten metal should have low viscosity, and molten pool should exist long enough to guarantee as good as possible mixing of the components.

The work done in this paper aims to optimize manufacturing of in-situ alloyed Ti6Al4V-1at.%Cu. The investigation is focused on development of optimal set of process parameters providing manufacturing of the high quality layers of the most homogeneous material. Obtained process parameters were used for manufacturing of 3D specimens, the microstructure and distribution of Cu in the surface and bulk material were studied by means of SEM-EDS. The results showed that in-situ approach is promising for manufacturing of novel advanced Ti alloy with incorporated antibacterial properties.

2. Materials and methods

In this study, argon atomized powders such as Ti6Al4V (ELI) containing 89.26 wt% of Ti, 6.31 wt% of Al, 4.09 wt% of V, 0.12% of O, and Cu of 99.9 % purity were used. Both powders were highly spherical in shape. The 10th, 50th and 90th percentiles of equivalent diameter (weighted by volume) were respectively 12.6 µm, 22.9 µm, 37 µm for Ti6Al4V (ELI) powder and 9.45 µm, 21.9 µm and 37.5 µm for Cu powder. To produce the Ti6Al4V-1 at.%Cu (1.38 wt%) powder mixture, the elemental Cu and Ti6Al4V(ELI) powders were mixed for 1 hour. Before the laser processing, the powders mixture was dried at 80°C for 2 hours without protective atmosphere, to increase powder flowability.

Specimens from the powder mixtures were manufactured on EOSINT M280 DMLS machine, operated at constant laser power 170 W at spot size of about 80 µm. Specimens were built up on the Ti6Al4V substrate. In order to determine the effect of a hatch distance and a scanning speed on the surface quality and distribution of elements in the in-situ sintered alloy, rectangular single layers with size 4.5x12 mm² were produced. Three scanning speeds (0.7 m/s, 1.0 m/s and 1.3 m/s) and four hatch distances (70 µm, 80 µm, 90 µm and 100 µm) were used. Single scan and rescan strategies were used to investigate influence of scanning strategy on surface roughness and homogeneity. Rescanning was done without shift in hatch distance in relation to the first scan.

The surface roughness of the samples was measured perpendicularly to the scanning direction with Surftest SJ-210 according to ISO 1997 standard.

To investigate distribution of elements in the bulk, 3D disc specimens of 10 mm in diameter and 5 mm in height were manufactured at 170 W laser power, 0.7 m/s scanning speed, 80 µm hatch distance and 30 µm layer thickness. Microhardness of the samples was measured at 200 g loading by Vickers's test in polished cross-sections cut perpendicular to the building direction (30 measurements for each cross-section).

Determination of chemical composition at the surface and 3D specimens was done by JEOL JSM-6610 scanning electron microscope with Thermo Scientific Ultra-dry energy-dispersive spectrometer and LEO 1350 FEG-SEM equipped with Oxford Instruments INCAx-sight EDX detector. Data on surface chemical composition should be interpreted with respect to the interaction volume of the electron beam and a material.

3. Results and discussion

Regular single tracks formed from stable molten pool is the most basic building block in the DMLS process. The optimization of formation of the molten pool and single track plays a major role in the quality and mechanical properties of the manufactured 3D object. The geometric characteristics of the DMLS tracks are mainly determined by material properties, energy input (laser power, spot size and scanning speed) and the thickness of the deposited powder layer. The depth of penetration into the substrate is determined

primarily by the power of laser beam, and the layer thickness causes the powder volume involved in melting process (Yadroitsev *et al.,* 2012).

In this study the laser power density, which is ratio of laser power to spot area, was constant. The highest powder layer thickness is a combination of the distance moved by the build platform in the Z-direction, and a roughness and shrinkage of the previously processed layer. The average surface roughness of reference Ti6Al4V samples perpendicular to the scanning direction at standard EOS process-parameters for 30 μm *Z*-movement of build platform, was found to be *Rz*=30.2±5.52 μm and *Ra*=6.9±1.37 μm. Thus, 60 μm powder layer thickness was used for the experiments with single layers.

Investigation of cross-sections showed that for 60 μm layer thickness and chosen process-parameters, total average remelted depth was about 60–70 μm for single layers sintered at different hatch distances. After rescanning, the total remelted depth increased to approximately 110 μm, Fig. 1. Defects such as porosity, delamination of layer and solidification cracks have not been found in DMLS single layers before and after rescanning. It confirms that selected manufacturing parameters are optimal and can guarantee metallurgical bonding and defect-free manufacturing of the Ti6Al4V-1 at. %Cu powders.
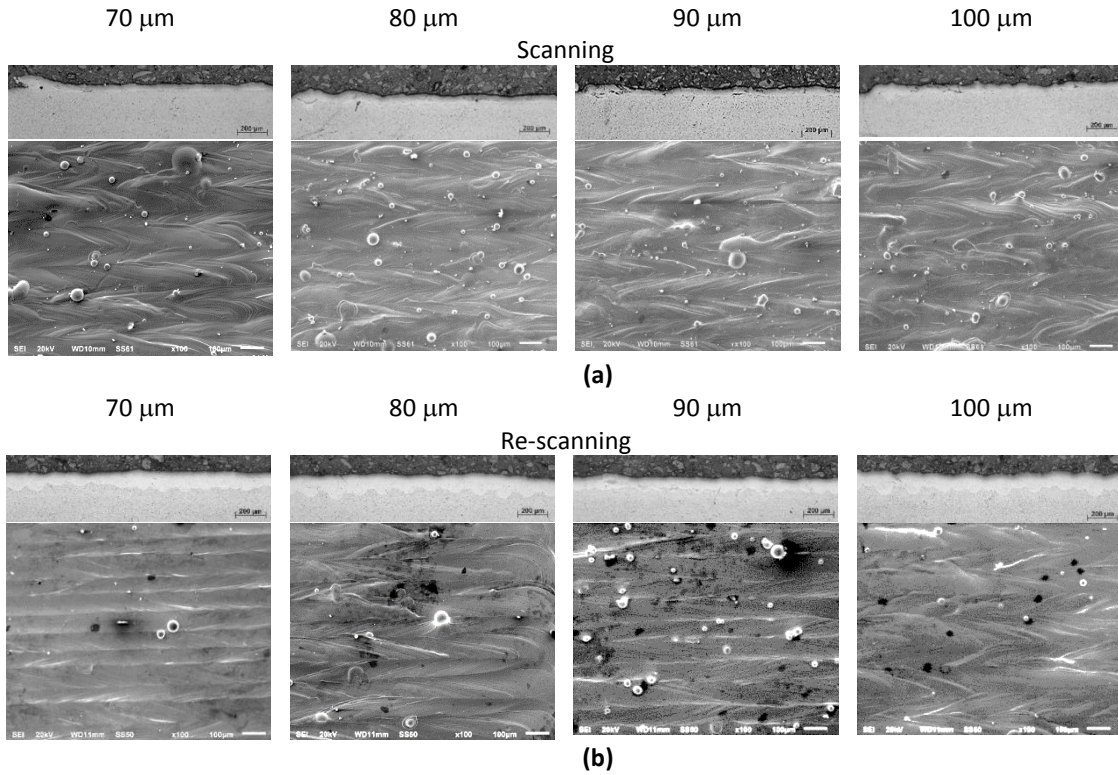

(a)

(b)

Fig. 1. Cross-sections and top view of DMLS surfaces from mixture Ti6Al4V (ELI) and 1 at.% Cu powders at laser power 170 W, scanning speed 1.0 m/s and 70-100 μm hatch distances: (a) single scan, (b) after rescanning.

While laser power and scanning speed have a major influence on single track geometry, hatch distance directly affects surface quality (hatch distance refers to the distance between centres of two neighbouring

single tracks). Due to the denudation effect, the first track is wider than the next one (Yadroitsev, 2009). The zone of powder consolidation does not have sufficient powder to form track with the same geometry. Optimal hatch distances are also essential for reducing process time and thermal cycling for DMLS. Investigation of DMLS single layers manufactured at different hatch distance showed that the surface roughness increased with an increase in hatch distance and scanning speed, Fig. 2. Surfaces of specimens manufactured at higher scanning speeds and higher hatch distances contained more satellites on the surface. It resulted in a dramatic decrease in the surface quality. Rescanning removed the satellites from the surfaces and showed some improvement of the surface quality. To further improvement the surface quality of in-situ DMLS alloying other rescanning strategies need to be also investigated. For example, shift in a hatch distance or change of a laser scanning direction at rescan could help in an optimization of the final surface roughness.
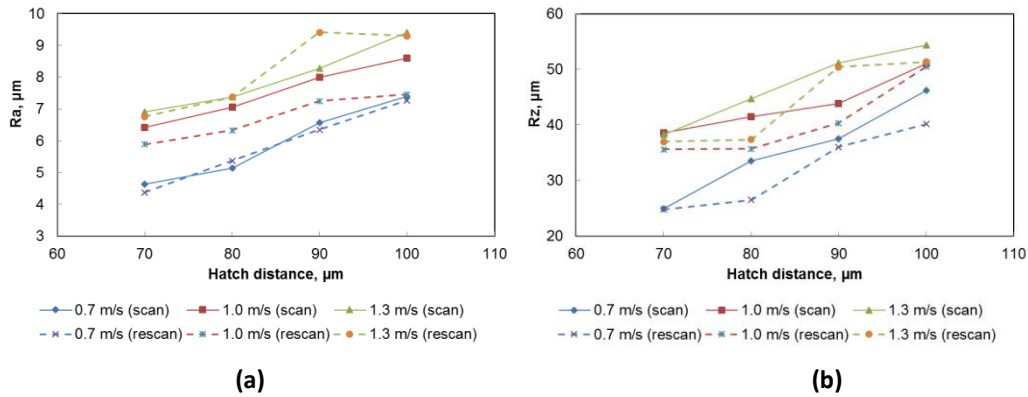

(a)   **(b)**

Fig. 2. Surface roughness of in-situ alloyed Ti6Al4V-1 at.%Cu at laser power 170 W, scanning speed 0.7-1.3 m/s and 70-100 μm hatch distances for a single scan and rescanning: (a) *Ra*, (b) *Rz*.

Since Cu introduces antibacterial properties to the bone – implant interface, a sufficient concentration and homogeneous distribution of Cu at the surface is required. In Figure 3, the surface concentration of Cu for in-situ Ti6Al4V-Cu alloyed layers is seen. For a single exposure at 0.7 m/s scanning speed and 70 μm hatch distance, the Cu concentration at the surface was 1.05%wt Cu. Content of Cu increased to 2.31%wt at scanning speed of 1.3 m/s and hatch distance and 100 μm. With an increase in scanning speed and hatch distance, concentration of Cu near the surface increased. The results with concentration of Cu closest to the nominal were observed at 0.7 m/s scanning speed.
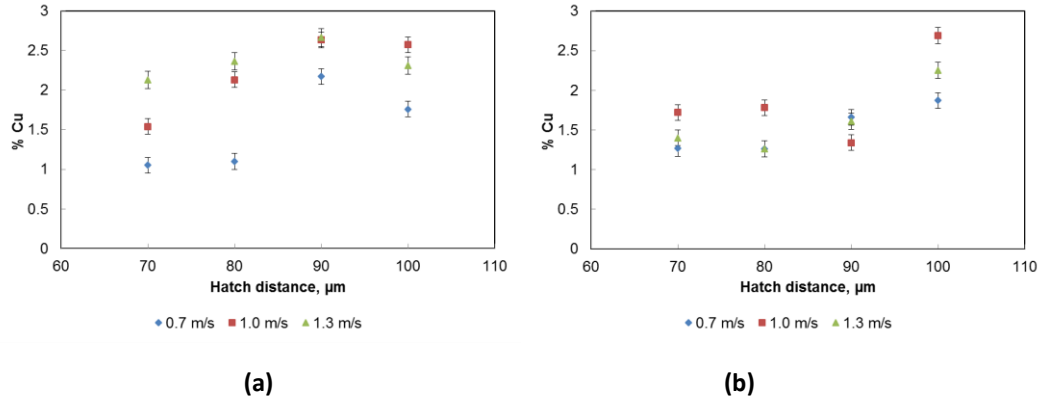
Fig. 3. SEM EDS data on the average wt.% of Cu at the DMLS surface of Ti6Al4V-1at%Cu powder at different scanning speeds and hatch distances, (a) single scan and (b) rescanning.

Investigation of homogeneity distribution of Cu in Ti6Al4V at the surface at various scanning speed (0.7-1.3 m/s) and hatch distances (70-100 µm) was performed by analysis of an EDS elemental maps. It was observed that after single scanning of the mixture Ti6Al4V and Cu powders, copper particles melted and created islands following solidification lines at the surface (Fig. 4a).
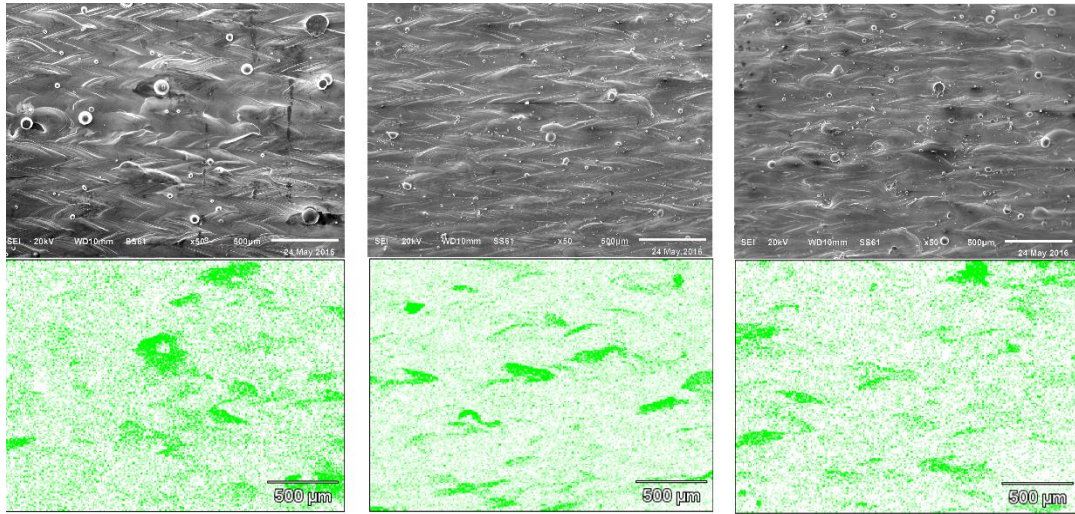
(a)
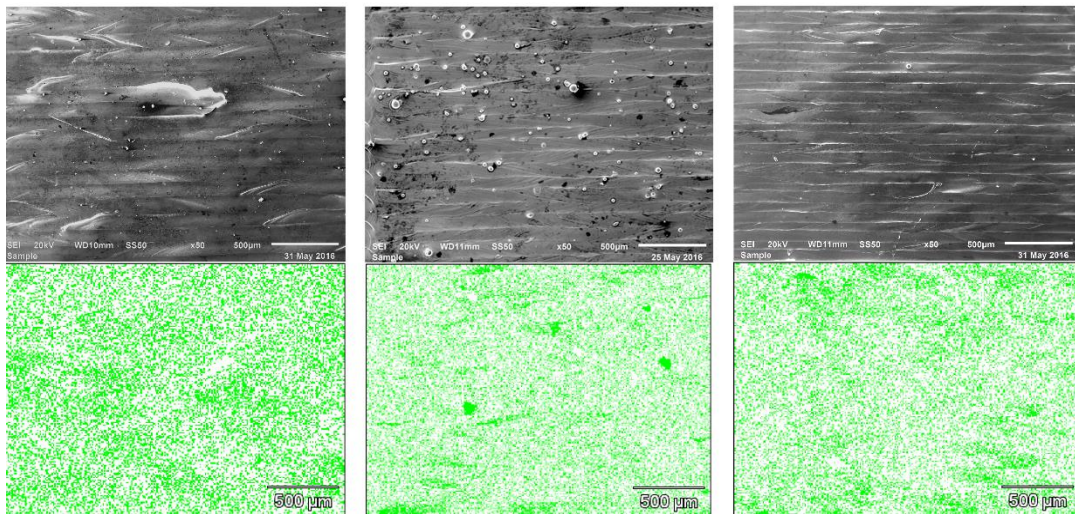
(b)

Fig. 4. Top view and corresponding copper distribution map by XRD spectra and in SE mode of DMLS surfaces of Ti6Al4V (ELI)-1 at.% Cu at laser power 170 W, scanning speeds 0.7-1.3 m/s and 90 µm hatch distances, (a) single scan, (b) after rescanning.

The rescanning strategy removed the copper segregations that formed at the peripheries of the single tracks. It could be due to repeating and complete re-melting of the material. Nevertheless, similarly to the results observed for the single scan strategy, at rescanning the Cu inhomogeneity slightly increased with scanning speed and hatch distance due to a decrease in energy input.

Observed effect of energy input on melting and surface of the Ti6Al4V-1%Cu alloy, could be explained taking into account the vast difference in material properties of Ti6Al4V alloy and Cu. Ti6Al4V and Cu have a specific heat capacity of 560 J/(kg×K) and 387 J/(kg×K), thermal conductivity of 7.2 W/(m×K) and 401 W/m×K, density of 4430 kg/m^3 and 8940 kg/m^3, melting temperature of 1922 K and 1356 K, latent heat of fusion of 370 kJ/kg and 205 kJ/kg. Taking into account latent heat of melting, heat capacity and density, energy for melting of unit volume of employed material can be estimated. For bulk Ti6Al4V and Cu this values are close: 4.03 J/mm^3 and 3.66 J/mm^3 respectively.

Estimated time of direct interaction laser beam–powder under laser spot size is $t_{D.I.}=d_0/V$, where d_0 is laser beam spot size and V is scanning speed. For 80 μm spot size and scanning speed V=0.7–1.3 m/s, time of laser-powder direct interaction is 114–61.5 μs. Temperature homogenization time in solid particles can be calculated as $t_{hom}=r^2/a$, where r is the particle radius and a is the thermal diffusivity of a bulk metal. This time is about 40 times higher for Ti6Al4V than for Cu. Estimation for 37 μm powder particle, the time of homogenization of Cu particle is 3 μs, while the time of homogenization of Ti6Al4V particle is 106 μs. Copper powder particles, therefore, is fused up first and then, transfers quickly heat to surrounding titanium alloy.

Viscosity in liquid Ti at temperatures of 1750-2050 K is 4.42 mPa×s, as it has been reported by Paradis *et al.* (2002). For pure liquid copper viscosity changes from 4.03 mPa×s at 1356 K to 1.96 mPa×s at 1950 K (Assasel *et al.*, 2010). Therefore, it is possible that at high scanning speeds (and, correspondingly, the short times of the interaction of laser radiation with powders), drops of liquid copper with low viscosity are distributed in a rather viscous liquid titanium alloy. Due to short interaction times, mixing is not sufficient for complete homogenisation and, Cu-rich regions are solidified in the matrix of the titanium alloy. Density of metals is another factor influencing homogeneity of the Ti6Al4V-Cu alloy. Liquid Cu has higher density and, in a case of incomplete mixing, can agglomerate near the fusion boundaries. Therefore, differences in density and viscosity could explain, Cu solidified as agglomerated areas at periphery of the molten bath.

Distribution of Cu in the bulk DMLS material was studied with SEM EDS on cross-sections of 3D specimens manufactured from the same initial powder mixture. Investigations have shown that Cu is quite well dissolved in the Ti alloy, although some areas enriched with Cu were observed. Fig. 5a and b illustrate distribution of Cu in the bulk material.

Cu-rich areas had characteristic shapes, which can easily be associated with molten pool boundaries (Fig. 6). Microstructure in these areas also differed from the regular surrounding structures (Fig. 7a). Regular microstructure has typical for martensite needle-like structure (Fig. 7b), commonly observed in Ti6Al4V manufactured by DLMS (Yadroitsev *et al,* 2014). Cu-rich regions could be divided to two groups, in one structure is also martensitic, in the others rather dendritic.

EDS analysis of chemical composition of areas with different microstructures showed that regular martensitic structure is not pure Ti6Al4V, but a material alloyed with Cu. Copper content in these areas varied in range of 1 – 1.5%. This concentration is quite close to the nominal concentration of pure Cu powder in the initial powder mixture. In the areas enriched with Cu but still having martensitic structure, even within one single area, concentration of Cu varied remarkably between 2 and 5 wt%. Highest concentration of Cu, up to 35 wt% was observed in areas that have different microstructure. Nevertheless, it is possible to conclude that the observed Cu-rich areas were not pure Cu, as concentration of Ti in those areas is high (Fig. 5d). No unmolten Cu particles were observed in the microstructure neither.

(a)

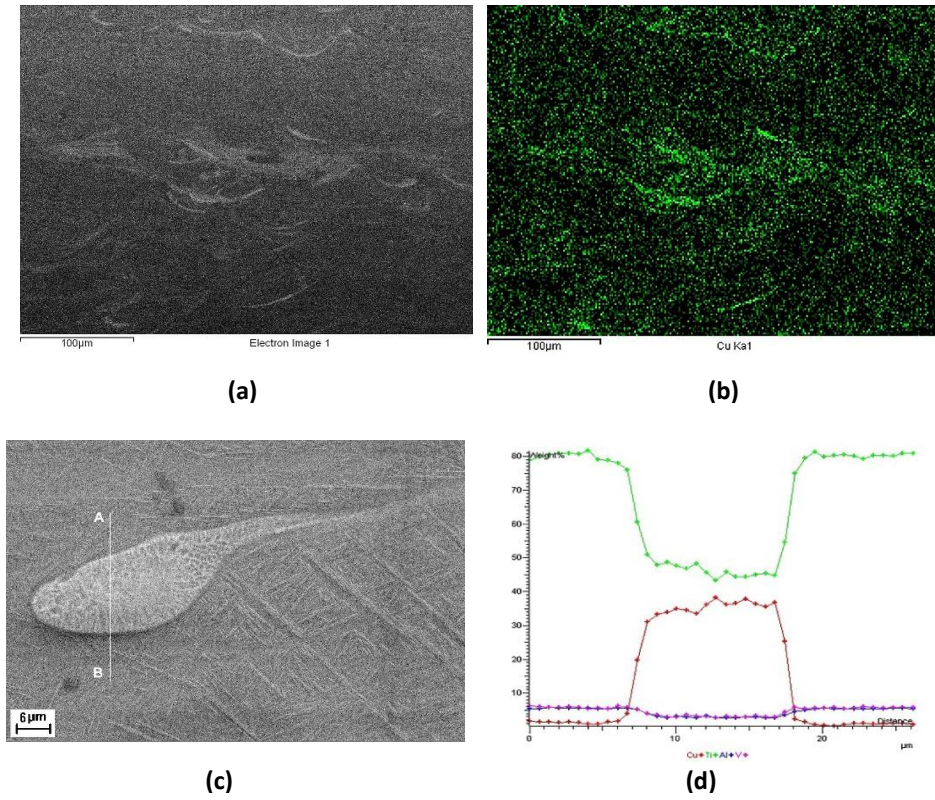**(b)**

(c)

(d)

Fig. 5. Copper distribution map by XRD spectra (a) electron image, (b) Cu EDS map illustration of typical microstructures, (c), Cu-rich area and (d) elemental concentration profiles of Ti, Al, V and Cu in the Cu-rich area in wt.%, data obtained along line AB in (c).
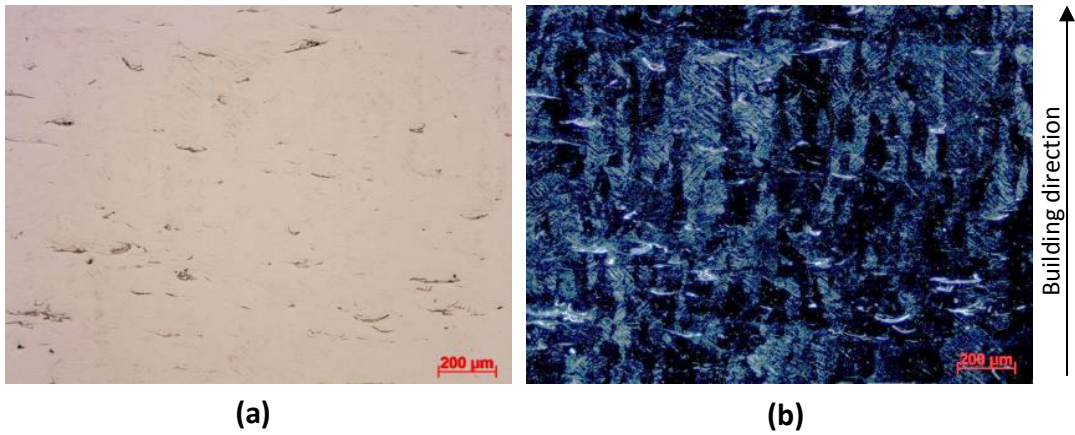

(a)

(b)

Building direction

Fig. 6. Microstructure of DMLS Ti6Al4V–Cu alloy (a) bright field and (b) dark field in optical microscope.

As it was discussed above, energy input was high enough to melt both Cu and Ti-alloy powders. Densities of molten Cu and Ti6Al4Al are different, and Cu-enriched regions have higher density. The fluid flows pushed heavier volumes of Cu-rich liquid to the peripheries of molten pool. If molten pool exists relatively long time, diffusion and convection support better mixing and formation of more homogeneous alloy. At higher scanning speeds, molten pool rapidly solidifies before copper can be sufficiently mixed and alloyed with the Ti6Al4V. Because of that somewhat higher surface inhomogeneity was observed in specimens manufactured with higher laser speed as at single and rescanning strategies. Therefore, it is possible to state that energy input was sufficient to remelt powder mixture completely, while observed inhomogeneity is a result of insufficient mixing due to different densities of Cu- and Ti-rich liquid.
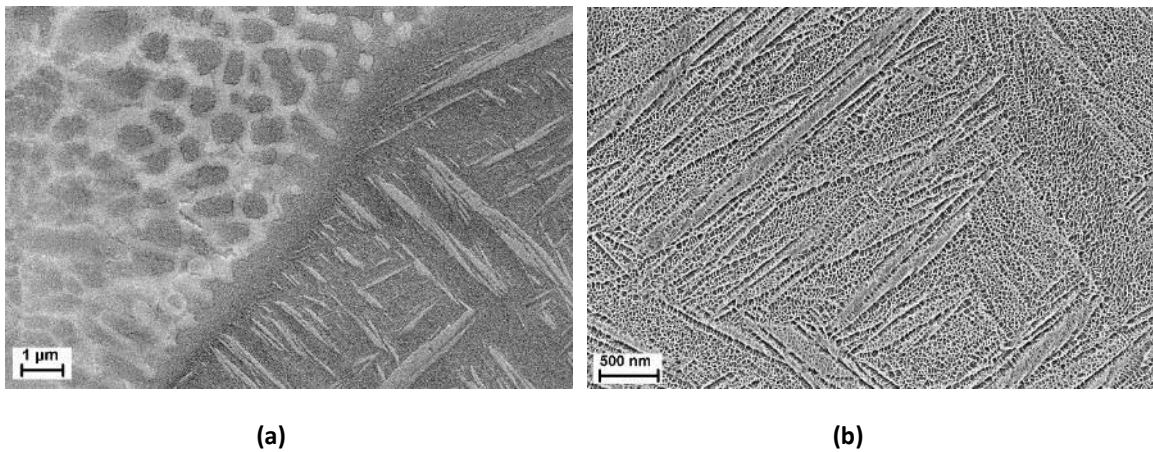

(a)   (b)

Fig. 7. Microstructure of DMLS Ti6Al4V–Cu alloy, (a) dendritic/cellular area with higher Cu content and, (b) martensitic structure with lower Cu content.

Basic mechanical properties of the Ti6Al4V-1 at.% Cu were characterized to understand an influence of alloying on mechanical performance of the in-situ alloyed material. As a reference, mechanical characteristics of Ti6Al4V manufactured with the same EOS equipment were used. Microhardness of as-built DMLS Ti6Al4V (ELI) samples was 383 ± 13 $HV_{0.2}$, while hardness of Ti6Al4V-1 at.% Cu was 456 ± 20 $HV_{0.2}$. Accordingly to the statistical analysis made with *t-test* ($p < 0.001$), observed increase in hardness was statistically significant. Strength characteristics showed the same trend. Ultimate tensile strength (UTS) of 1243 ± 49 MPa of the as-built non-polished mini-samples produced from Ti6Al4V (ELI) has been reported (van Zyl et al., 2016). In-situ alloying with Cu led to the substantial increase of ultimate tensile strength up to 1550 ± 126 MPa. Cu is also well-known as a beta stabilizer in titanium alloys. Therefore, it is possible that in the areas with higher Cu concentration, an intermetallic Ti_2Cu phase and/or Ti-beta phase were formed. Guo *et al.* (2017) have found presence of hard intermetallic compounds in DMLS Ti6Al4V–xCu alloys after water quenching. They reported that a relative diffraction intensity of Ti_2Cu phase gradually increased with the Cu contents. Authors also suggested that the intermetallic phase in Ti6Al4V–xCu alloys could result in higher values of microhardness and UTS and, at the same time, some embrittlement of in-situ alloyed samples. Nevertheless, mechanisms behind strengthening effect of Cu in in-situ alloyed Ti6Al4V have to be

investigated more thoroughly and be proven by experimental investigations and phase identifications in sintered DMLS material. Solid solution strengthening effect of Cu in titanium alloy and refinement of martensite lamella are the other possible factors influencing observed enhance in hardness and UTS in the investigated Ti6Al4V–Cu alloy.

4. Conclusions

In-situ alloying of Ti6Al4V (ELI) and 1at.% Cu powder was successfully performed utilizing DMLS. Produced single layers exhibited no signs of porosity, delamination, or solidification cracks. The surface quality of the produced layers was improved with a decrease in scanning speed and hatch distance.

The applied rescanning strategy removed surface satellite particles, improving the surface quality. Rescanning had a profound improvement on surface homogeneity and surface composition; this is attributed to the complete re-melting of the single layer. It can be concluded that the surface quality and homogeneous surface distribution of Cu in the in-situ alloyed Ti6Al4V-1at.%Cu can be improved by decreasing the scanning speed and hatch distance, within the optimal process parameters, or applying the rescanning strategy.

In the bulk material some inhomogeneity also observed. Areas of enhanced Cu concentrations are associated with fusion boundaries. Enrichment with Cu differs from area to area, nevertheless, surrounding materials contains about 1at% Cu which indicated, although incomplete but sufficient alloying of Ti6Al4V with Cu in-situ at DLMS of powder mixtures.

Acknowledgements

References

Assael M.J., Kalyva A.E., Antoniadis K.E., Banish R.M., Egry I., Quested P.N., Wu, J., Kaschnitz E., Wakeham W.A., 2010. Reference Data for the Density and Viscosity of Liquid Copper and Liquid Tin", J. Phys. Chem. Ref. Data, 39, pp. 033105:1-9

Dadbakhsh, S. and Hao, L., 2014. Effect of layer thickness in selective laser melting on microstructure of Al/5 wt.% Fe2O3 powder consolidated parts. The Scientific World Journal, 2014, pp. 1-10.

Fischer, M., Joguet, D., Robin, G., Peltier, L. and Laheurte, P., 2016. In situ elaboration of a binary Ti–26Nb alloy by selective laser melting of elemental titanium and niobium mixed powders. Materials Science and Engineering, 62, pp. 852-859.

Geetha, M., Singh, A.K., Asokamani, R. & Gogia, A.K., 2009. Ti based biomaterials, the ultimate choice for orthopaedic implants–a review. Progress in Materials Science, 54(3), pp.397–425.

Guo S, Lu Y, Wu S, Liu L, He M, Zhao C, Gan Y, Lin J, Luo J, Xu X, Lin J., 2017. Preliminary study on the corrosion resistance, antibacterial activity and cytotoxicity of selective-laser-melted Ti6Al4V-xCu alloys. Materials Science & Engineering. C, Materials for Biological Applications. 72: 631-640.

Jung, C. Straumann, L., Kessler, A., Pieles, U. and de Wild, M., 2014. Antibacterial copper deposited onto and into the oxide layer of titanium implants, BioNanoMat. 15 (2014) S180.

Kinnear, A.W., 2015. Direct metal laser sintering of multiple material structures for biomedical applications, MTech thesis, Central University of Technology, Free State, South Africa, pp. 121.

Krakhmalev, P. and Yadroitsev, I., 2014. Microstructure and properties of intermetallic composite coatings fabricated by selective laser melting of Ti–SiC powder mixtures. Intermetallics, 46, pp.147-155.

Nan, L., Yang, W.C., Liu, Y.Q., Xu, H., Li, Y., Lu, M.Q. and Yang, K., 2008. Antibacterial mechanism of copper-bearing antibacterial stainless steel against E. coli. Journal of Materials Science and Technology, 24, pp. 197–201.

Niinomi, M., 2008. Mechanical biocompatibilities of titanium alloys for biomedical applications. Journal of the Mechanical Behavior of Biomedical Materials, 1, pp.30–42.

Paradis P.-F., Ishikawa, T., and Yoda, S., 2002. Non-Contact Measurements of Surface Tension and Viscosity of Niobium, Zirconium, and Titanium Using an Electrostatic Levitation Furnace. International Journal of Thermophysics, 23 (3), pp. 825–842.

Shirai, T., Tsuchiya, H., Shimizu, T., Ohtani, K., Zen, Y. and Tomita, K. (2009). Prevention of pin tract infection with Titanium-Copper alloys, J. Biomed. Mater. Res. B Appl. Biomater. 91B, pp 373-380.

van Zyl I., Moletsane M., Krakhmalev P., Yadroitsava I., Yadroitsev I., 2016. Validation of miniaturised tensile testing on DMLS TI6Al4V (ELI) specimens. The South African Journal of Industrial Engineering, 27 (3): 192-200.

Vrancken, B., Thijs, L., Kruth, J.P. and Van Humbeeck, J., 2014. Microstructure and mechanical properties of a novel β titanium metallic composite by selective laser melting. Acta Materialia, 68, pp.150-158.

Yadroitsava I., Els J., Booysen G., Yadroitsev I., 2015. Peculiarities of single track formation from TI6AL4V alloy at different laser power densities by SLM. The South African Journal of Industrial Engineering, 26 (3): 86-95.

Yadroitsev I., Krakhmalev P., Yadroitsava, I., 2014. Selective laser melting of Ti6Al4V alloy for biomedical applications: temperature monitoring and microstructural evolution, Journal of Alloys and Compounds. 583, 404-409.

Yadroitsev, I., 2009. Selective laser melting: direct manufacturing of 3D-objectsby selective laser melting of metal powders. Saarbrucken: LAP Lambert Academic Publishing AG & Co. KG; pp. 307.

Yadroitsev, I., Yadroitsava, I., Bertrand, Ph. and Smurov, I., 2012. Factor analysis of selective laser melting process parameters and geometrical characteristics of synthesized single tracks. Rapid Prototyping Journal, 18 (3), pp. 201-208.